

# Time-Delayed *In Vivo* Assembly of Subunit *a* into Preformed *Escherichia coli* F<sub>O</sub>F<sub>1</sub> ATP Synthase

Britta Brockmann, Kim Danielle Koop genannt Hoppmann, Henrik Strahl,\* Gabriele Deckers-Hebestreit

Abteilung Mikrobiologie, Fachbereich Biologie/Chemie, Universität Osnabrück, Osnabrück, Germany

*Escherichia coli* F<sub>O</sub>F<sub>1</sub> ATP synthase, a rotary nanomachine, is composed of eight different subunits in a  $\alpha_3\beta_3\gamma\delta\epsilon ab_2c_{10}$  stoichiometry. Whereas F<sub>O</sub>F<sub>1</sub> has been studied in detail with regard to its structure and function, much less is known about how this multisubunit enzyme complex is assembled. Single-subunit *atp* deletion mutants are known to be arrested in assembly, thus leading to formation of partially assembled subcomplexes. To determine whether those subcomplexes are preserved in a stable standby mode, a time-delayed *in vivo* assembly system was developed. To establish this approach, we targeted the time-delayed assembly of membrane-integrated subunit *a* into preformed F<sub>O</sub>F<sub>1</sub> lacking subunit *a* (F<sub>O</sub>F<sub>1</sub>-*a*) which is known to form stable subcomplexes *in vitro*. Two expression systems (*araBADp* and *T7p-laco*) were adjusted to provide compatible, mutually independent, and sufficiently stringent induction and repression regimens. In detail, all structural *atp* genes except *atpB* (encoding subunit *a*) were expressed under the control of *araBADp* and induced by arabinose. Following synthesis of F<sub>O</sub>F<sub>1</sub>-*a* during growth, expression was repressed by glucose/D-fucose, and degradation of *atp* mRNA controlled by real-time reverse transcription-PCR. A time-delayed expression of *atpB* under *T7p-laco* control was subsequently induced *in trans* by addition of isopropyl- $\beta$ -D-thiogalactopyranoside. Formation of fully assembled, and functional, F<sub>O</sub>F<sub>1</sub> complexes was verified. This demonstrates that all subunits of F<sub>O</sub>F<sub>1</sub>-*a* remain in a stable preformed state capable to integrate subunit *a* as the last subunit. The results reveal that the approach presented here can be applied as a general method to study the assembly of heteromultimeric protein complexes *in vivo*.

The F<sub>O</sub>F<sub>1</sub> ATP synthase catalyzes the formation of ATP from ADP and inorganic phosphate by utilizing the energy stored in the ion motive force of the cytoplasmic membrane. In many bacteria, the reaction is reversible dependent on the physiological conditions and can generate a transmembrane ion gradient at the expense of ATP. In *Escherichia coli* ATP synthase, the membrane-embedded F<sub>O</sub> complex ( $ab_2c_{10}$ ) couples proton translocation to ATP synthesis and hydrolysis within the peripherally associated catalytic F<sub>1</sub> complex ( $\alpha_3\beta_3\gamma\delta\epsilon$ ) via a rotary mechanism. The transmembrane flow of protons through two half-channels of subunit *a* drives the rotation of the rotor  $c_{10}\gamma\epsilon$  due to protonation and deprotonation of carboxyl groups of the subunit *c* ring. Subunit  $\gamma$ , which rotates inside a molecular bearing composed of the alternately arranged  $\alpha_3\beta_3$  hexamer, generates cyclic conformational changes due to its eccentric rotation within the three catalytic nucleotide binding sites, thereby allowing the synthesis of ATP. The  $\alpha_3\beta_3$  hexamer of F<sub>1</sub>, as well as subunit *a* of F<sub>O</sub>, is connected to the stator stalk composed of  $b_2\delta$ , thereby forming a stabilizing stator part counteracting the rotating  $c_{10}\gamma\epsilon$  unit (1, 2).

Whereas ample knowledge is available regarding the insertion of F<sub>O</sub> subunits into the membrane, only a few facts are at hand as to how a functional F<sub>O</sub>F<sub>1</sub> complex is assembled in *E. coli*. The F<sub>O</sub>F<sub>1</sub> complex consists of 22 polypeptide chains, which are expected to contain interaction areas with various affinities. Insertion of subunit *c* into the membrane involves YidC insertase and subunit *b* is dependent on the SecYEG translocon and the signal recognition particle pathway (Ffh), whereas subunit *a* requires all three systems for membrane insertion (3–5). In addition, subunits *b* and *c* are both essential for a stable incorporation of subunit *a* into the membrane *in vivo* (6, 7); otherwise, subunit *a* is rapidly degraded as a substrate of the membrane-integrated, ATP-dependent metalloprotease FtsH (8, 9). In contrast, subunits *b* and *c* insert into the membrane independently of other F<sub>O</sub> subunits (6) and the  $c_{10}$

ring is formed in a manner independent of the presence of other F<sub>O</sub>F<sub>1</sub> subunits (10). For the Na<sup>+</sup>-pumping F<sub>O</sub> complexes of *Protonigenium modestum* and *Acetobacterium woodii*, a chaperone-like assistance of AtpI for the formation of the *c* ring has been shown to be essential (11–13). However, in *E. coli*, AtpI, a membrane-integrated protein of 14 kDa present in the membrane in substoichiometric amounts compared to F<sub>O</sub>F<sub>1</sub> (14, 15), is not required for the assembly of a functional ATP synthase (16). However, studies of the H<sup>+</sup>-translocating ATP synthase of alkaliphilic *Bacillus pseudofirmus* OF4 revealed slightly reduced stability of the rotor as well as reduced ATPase activity (17). In the absence of subunit *a*, membrane-bound ATPase activities indicate an assembly of F<sub>1</sub> to the subunit *c* ring (6), as has also been proposed for the assembly of the ATP synthase of yeast mitochondria (18, 19). The minimal catalytic unit stably present in the cytoplasm is composed of  $\alpha_3\beta_3\gamma$  (20, 21), and complex formation of subunit  $\alpha$  with other F<sub>1</sub> subunits is a prerequisite for the binding of subunit  $\delta$  to the N-terminal region of subunit  $\alpha$  (22). In the case of both thermophilic *Bacillus* PS3 and human  $p^0$  cells, a stable F<sub>O</sub>F<sub>1</sub> subcomplex

Received 23 April 2013 Accepted 3 July 2013

Published ahead of print 8 July 2013

Address correspondence to Gabriele Deckers-Hebestreit, deckers-hebestreit@biologie.uni-osnabrueck.de.

\* Present address: Henrik Strahl, Centre for Bacterial Cell Biology, Institute for Cell and Molecular Biosciences, Newcastle University, Newcastle upon Tyne, United Kingdom.

Supplemental material for this article may be found at <http://dx.doi.org/10.1128/JB.00468-13>.

Copyright © 2013, American Society for Microbiology. All Rights Reserved.  
doi:10.1128/JB.00468-13

lacking subunit *a* can be purified (23–25), clearly indicating that the F<sub>1</sub> subunits are associated with the subunit *c* ring and the peripheral stalk prior to attachment of subunit *a*.

The analysis of partially assembled subcomplexes is a prerequisite for defining the sequence of events in the assembly process of the ATP synthase. In single-subunit knockout or deletion mutants, in which the synthesis of one of the subunits of the heteromultimeric complex is prevented, an accumulation of partially assembled subcomplexes can be expected until a status is reached at which the missing subunit has to be inserted into the preformed ensemble (6, 26, 27). To determine the stability of those preformed, partially assembled subcomplexes and, furthermore, to determine the preservation of their native molecular conformation in a standby mode ready for use, an *in vivo* assembly system was developed in which the missing subunit is synthesized in a time-delayed mode, thereby excluding *de novo* synthesis of F<sub>0</sub>F<sub>1</sub>. In addition, due to the formation of those subcomplexes under physiological conditions within the living cell, disintegration of unstable subcomplexes formed as intermediate states is minimized, since manipulations such as cell disruption by sonication or high shearing forces are avoided.

To establish this new approach, we targeted the time-delayed assembly of membrane-integrated subunit *a* into preformed F<sub>0</sub>F<sub>1</sub> complexes lacking subunit *a* (F<sub>0</sub>F<sub>1</sub>-*a*) *in vivo* as an example. For F<sub>0</sub>F<sub>1</sub> of thermophilic *Bacillus* PS3, it has been shown that a functional *in vitro* reconstitution of both components into liposomes was successful (23, 24). In detail, we established a system in which all structural *atp* genes except *atpB* (*atpEFHAGDC*) were expressed under the control of the tightly regulated *araBAD* promoter by induction with arabinose (28, 29). After synthesis of F<sub>0</sub>F<sub>1</sub>-*a* during growth, further expression of *atpEFHAGDC* was completely repressed by the catabolite repressor glucose and the anti-inducer D-fucose (28, 30). Complete degradation of the *atp* mRNA was controlled by real-time reverse transcription-PCR (RT-PCR), and the expression of *atpB* encoding subunit *a* was subsequently started *in trans* via induction of a isopropyl-β-D-thiogalactopyranoside (IPTG)-controlled T7-*laco* promoter (31). The time delay of the IPTG-controlled expression is the centerpiece of the *in vivo* assembly system introduced, since a complete degradation of the *atp* mRNA of the *araBADp*-controlled expression prior to IPTG induction is essential to exclude the formation of a functional enzyme complex by *de novo* protein synthesis from still-existing mRNA. In addition, the stringent repression of the T7-*laco* promoter prior to induction was controlled. The formation of a functionally assembled F<sub>0</sub>F<sub>1</sub> complex was verified by N,N'-dicyclohexylcarbodiimide (DCCD)-sensitive ATPase activity and ATP-driven proton translocation as well as ATP synthesis, clearly demonstrating that all subunits of F<sub>0</sub>F<sub>1</sub>-*a* remain in a preformed state with stability comparable to that of the wild-type (WT) enzyme and are ready to integrate subunit *a* as the last subunit into the enzyme complex.

## MATERIALS AND METHODS

**Mutagenesis.** In most cases, a two-step PCR method that utilizes two mutagenic primers (see Table S1 in the supplemental material) and two wild-type primers with the corresponding restriction sites was used to generate stop codons in *atpB* (*aY11amber* or *aW231opal*) or an *atpB* deletion, which comprises the *atpB* coding region as well as the intergenic region between *atpI* and *atpB* (Table 1; see also Table S2 in the supplemental material). In addition, a KpnI site was introduced 49 bp upstream

TABLE 1 *E. coli* strain and plasmids used in this study

Strain or plasmid <sup>a</sup>	Genotype/description <sup>b</sup>	Reference or source
<i>E. coli</i> strain		
DK8	<i>hfrPO1 bglR thi-1 relA1 ilv::Tn10</i> (Tet <sup>r</sup> ) <i>ΔatpBEFHAGDC</i>	35
Plasmids		
pBAD33	Cm <sup>r</sup> <i>araC pACYC184 ori</i>	29
pBAD33.atp	pBAD33:: <i>atpBEFHAGDC</i>	This study
pBAD33.Δa	pBAD33:: <i>atpBEFHAGDC</i> , <i>aW231end</i>	This study
pBAD33.Δa2	pBAD33:: <i>atpBEFHAGDC</i> , <i>aY11end</i>	This study
pBAD33.Δa3	pBAD33:: <i>atpEFHAGDC</i>	This study
pBWU13	Ap <sup>r</sup> pMB1 <i>ori atpI' BEFHAGDC</i>	66, 67
pET-22b	Ap <sup>r</sup> <i>lacI</i> pMB1 <i>ori</i>	Novagen
pET22-atpB	pET-22b:: <i>atpB</i> , start codon ATG	This study
pET22-atpB-GTG	pET-22b:: <i>atpB</i> , start codon GTG	This study
pET22-atpB-TTG	pET-22b:: <i>atpB</i> , start codon TTG	This study
pJGA1	Ap <sup>r</sup> pMB1 <i>ori atpI' EFHAGDC</i>	This study
pT7POL26	Kan <sup>r</sup> T7 gene 1 <i>lacI</i> pSC101 <i>ori</i>	51

<sup>a</sup> Construction of plasmids is described in Table S2 in the supplemental material.

<sup>b</sup> Ap, ampicillin; Cm, chloramphenicol; Kan, kanamycin; Tet, tetracycline; T7 gene 1, T7 RNA polymerase.

of the stop codon of *atpI*, i.e., downstream of the weak, constitutive *atp* promoter P3 (32). The *atp* genes present in pKH4 derivatives (33, 34) carrying one of the different modifications of *atpB* were subsequently cloned into the multiple-cloning site of pBAD33 via KpnI within *atpI* and XbaI being present 320 bp downstream of the 3' end of the *atpC* gene, thereby allowing its expression under the control of the tightly regulated promoter *araBADp*. The *atpB* gene carrying variations in the start codon was cloned into plasmid pET-22b as described here (Table 1; see also Table S2 in the supplemental material). The presence of each mutation was confirmed by DNA sequencing.

(The following generalizations were chosen to facilitate reading. The term F<sub>0</sub>F<sub>1</sub> is used for *E. coli* DK8 cells bearing plasmids pBAD33.atp, pET-22b, and pT7POL26 as well as for the enzyme complex synthesized by these cells, whereas the term F<sub>0</sub>F<sub>1</sub>-*a* is used for DK8 cells bearing plasmids pBAD33.Δa3, pET22-atpB-GTG, and pT7POL26 as well as for the enzyme complex lacking subunit *a*. The term F<sub>0</sub>F<sub>1</sub>-*a* + *a* denotes enzyme complexes obtained after time-delayed incubation of cells containing F<sub>0</sub>F<sub>1</sub>-*a* with IPTG during growth. The term WT [wild type] is used for ATP synthase complexes synthesized by DK8/pBWU13.)

**Bacterial strains and growth conditions.** The genotype of *E. coli* strain DK8 (35) is described in Table 1. DK8 transformed with three different plasmids [pBAD33.atp, pET-22b, and pT7POL26 (F<sub>0</sub>F<sub>1</sub>)] or its derivatives (Table 1) were grown in 700 ml Luria-Bertani (LB) medium (36) at 37°C with 100 μg/ml ampicillin (Ap), 30 μg/ml chloramphenicol (Cm), and 50 μg/ml kanamycin (Kan) as selection markers. In each case, prior to cell growth, the LB medium was incubated for 10 to 16 h with 10 U/ml β-galactosidase (β-Gal) from *Kluyveromyces lactis* (Sigma G-3665), thereby degrading the lactose present in various concentrations in the yeast extract used for preparing LB medium (37). Additionally, the medium was supplemented with 0.03% (wt/vol) arabinose for induction of *araBADp*-controlled *atp* genes prior to inoculation of the medium to an optical density (OD; measured at 578 nm) of 0.05 with overnight cultures also grown in the presence of 0.03% (wt/vol) arabinose. At OD = 0.3, the *araBAD* promoter was repressed by the simultaneous addition of 0.5% (wt/vol) glucose and 0.045% (wt/vol) D-fucose (28, 29). After natural degradation of the *atp* mRNA during an additional incubation time of 30 min, the expression of *atpB*, being under the control of the IPTG-inducible T7 promoter, and of T7 *gene1* coding for T7 RNA polymerase, being under the control of an IPTG-inducible T5N25 promoter, was induced by addition of 0.1 mM IPTG for 1 h.

**RNA extraction, cDNA synthesis, and real-time RT-PCR.** Cells ( $2.5 \times 10^8$ ) of *E. coli* strain DK8 transformed with three different plasmids [pBAD33.atp, pET-22b, and pT7POL26 ( $F_0F_1$ )] or its  $F_0F_1$ -*a* derivatives, e.g., pBAD33.Δa3, pET22-atpB-GTG, and pT7POL26, were mixed with 2 vol of RNAprotect bacteria reagent (Qiagen), incubated for 5 min at room temperature, harvested at  $5,000 \times g$ , and stored at  $-20^\circ\text{C}$ . The amount of cell culture needed was calculated according to the determination of Neidhardt et al. (38) that 1 ml of cells contains  $10^9$  viable cells at OD = 1.0. The different steps necessary were performed essentially as described by Strahl and Greie (39) with slight modifications. Total RNA was isolated by use of an RNeasy minikit (Qiagen) following the instructions of the supplier. RNA was diluted with RNase-free water to obtain 10 μg/ml and subsequently treated with DNase I (New England BioLabs) as indicated by the supplier to remove residual DNA contaminations prior to reverse transcription. Total RNA (65 ng) was reverse transcribed by use of a RevertAid First Strand cDNA synthesis kit (Fermentas) using the random hexamer primers supplied. For detection of gene expression levels, real-time RT-PCR was performed on a Bio-Rad iCycler with Bio-Rad iQ-SYBR green Supermix, 1 μl of cDNA, and 0.2 nmol of each primer. The primer pairs *atpE'F'* (1 and 2) and *atpA* (3 and 4) (see Table S1 in the supplemental material) generate PCR products of approximately 200 bp. PCR was performed using an initial denaturation at  $96^\circ\text{C}$  for 1 min followed by 40 cycles of denaturation at  $96^\circ\text{C}$  for 15 s, annealing at  $59^\circ\text{C}$  for 30 s, and extension at  $72^\circ\text{C}$  for 20 s. The calculated threshold cycle ( $C_T$ ) values were normalized against  $C_T$  values of reactions using a primer pair annealing within the *rpsL* gene as the housekeeping gene (primers 5 and 6; see Table S1 in the supplemental material) and analyzed with the program iCycler from Bio-Rad. As negative controls, reaction mixtures containing  $\text{H}_2\text{O}$  (no template) or DNase I-treated RNA (without reverse transcription) were included. The data represent average values obtained in three independent measurements.

**Preparative procedures.** Inverted membrane vesicles were prepared according to Krestakies et al. (40) using 50 mM Tris-HCl (pH 7.5)–10 mM  $\text{MgCl}_2$ –10% (vol/vol) glycerol as a buffer system.

**Analytical procedures.** Protein concentrations were determined with the bicinchoninic acid (BCA) assay as recommended by the supplier (Pierce). Proteins were dissolved in SDS-PAGE sample loading buffer (41) and separated by SDS-PAGE using 10% separating gels (42) with a PageRuler prestained protein ladder (Fermentas) as the standard. Immunoblotting was performed according to Birkenhäger et al. (43) using 10 mM  $\text{NaHCO}_3$ –3 mM  $\text{Na}_2\text{CO}_3$  (pH 9.9)–20% (vol/vol) methanol as the transfer buffer (44). Blot membranes were incubated with corresponding primary antibodies raised in mice or rabbits (see figure legends), with IRDye800DX-labeled goat-anti-mouse IgG (H+L) or IRDye700DX-labeled goat anti-rabbit IgG (H+L) (Rockland or LI-COR) as the secondary antibody, and were finally detected with a two-channel Odyssey infrared detection system (LI-COR). Both secondary antibodies are affinity purified for low crossreactivities with serum proteins of other species and, therefore, allowed the simultaneous detection of fluorescence (shown in red for IRDye700DX and in green for IRDye800DX) after immunodecoration of two proteins on one blot membrane.

DCCD-sensitive ATPase activities of membrane vesicles were determined as described previously (45). ATP-driven proton translocation via 9-amino-6-chloro-2-methoxyacridine (ACMA; Sigma A-5806) fluorescence quenching was performed according to Deckers-Hebestreit et al. (46) using only half of the volume specified and 400 μg membrane protein. In the case of NADH-driven proton translocation, 200 μg of inverted membrane vesicles was applied. As an uncoupler, 20 μl of a saturated ammonium sulfate solution was used. ATP synthesis activity was measured at  $37^\circ\text{C}$  with 30 μg of membrane vesicle protein in 500 μl of buffer (25 mM Tris-HCl [pH 7.5], 5 mM  $\text{MgCl}_2$ , 10% [vol/vol] glycerol, 5 mM ADP, 5 mM  $\text{K}_2\text{HPO}_4$ ) (47). The reaction was initiated by addition of 2 mM NADH and terminated after 0, 1, 2, and 3 min with 50 μl of 0.5 M trichloroacetic acid. Aliquots (1 μl) of the reaction mixture were diluted 100-fold in 0.1 M Tris-acetate (pH 7.8)–2 mM EDTA. In 10-μl samples of

this dilution, ATP was determined luminometrically using a Promega Enliten luciferin/firefly luciferase system. Due to contamination of ADP with ATP, ADP was purified via anion-exchange chromatography on a 5 ml Hi-Trap-DEAE FF column (GE Healthcare). ADP (50 mg) was dissolved in 20 mM Tris-acetate (pH 8.5), loaded onto the column, and eluted with a linear NaCl gradient (0 to 400 mM). The eluted ADP was directly used for buffer preparation. The data represent average values obtained in three independent measurements.

## RESULTS

**$F_0F_1$ -*a* is known to form a stable subcomplex.** Consistent with previous work (6, 23, 48), we observed stable synthesis of all  $F_0F_1$  subunits except subunit *a* in cells of single-subunit knockout (*aW231end* or *aY11end*; data not shown) or deletion ( $\Delta$ *atpB*; Fig. 1A) mutants expressing the *atp* genes from the corresponding plasmids. Evidence for a stable subcomplex formation resulted from the observation that  $F_0F_1$ -*a* can be isolated via a His<sub>6</sub> tag fused to the N terminus of subunit β from *E. coli* membranes (68). In our setup for the *in vivo* approach, the single-subunit deletion mutant  $\Delta$ *atpB* was applied, since in the knockout *aY11end* mutant the amount of  $F_0F_1$  protein present in the cell is comparably low (data not shown), probably due to a polar effect on the expression of the *atp* genes located downstream of *atpB*. On the other hand, the *aW231end* mutant, well described in the literature (6, 49, 50), showed a truncated subunit *a* in immunoblots, when expression of the mutated *atp* operon was under the control of the *araBAD* promoter. In contrast, during constitutive expression under the control of the weak *atp* promoter P3, the truncated subunit *a* product could not be detected (data not shown), a discrepancy that has been previously discussed in detail (6).

In membrane vesicles of the *atpB* deletion mutant (DK8/pBAD.Δa3), ATPase activities comparable to those seen with the corresponding wild-type enzyme (DK8/pBAD33.atp) were observed (Fig. 1B), an activity that can be detected only when catalytically active  $F_1$  or at least an  $\alpha_3\beta_3\gamma$  subcomplex has been bound to membrane-integrated  $F_0$  subunits, indicating the assembly of a stable subcomplex. Similar results have been obtained by Hermolin and Fillingame (reference 6 and references therein), whereas comparable studies on *Bacillus* PS3  $F_0F_1$ -ATP synthase revealed that no ATPase activity could be detected in the absence of subunit *a* (23). Nevertheless, as expected, no ATP-driven proton translocation measured with the pH-sensitive dye ACMA could be observed due to the absence of the two half-channels within subunit *a* essential to enable proton translocation across the cytoplasmic membrane (Fig. 1C). Therefore, ATP-driven proton translocation has been used as the measure to discriminate between  $F_0F_1$ -*a* and intact  $F_0F_1$ .

***In vivo* system for time-delayed assembly of membrane-integrated subunit *a* into preformed  $F_0F_1$ -*a*.** The system used is based on the combination of two tightly regulated expression systems that work almost independently of each other and can be induced as well as completely repressed. For genes *atpEFHAGDC*, expression was controlled by the *araBAD* promoter (*araBADp*) chosen due to its specificity for induction with arabinose and, more importantly, its tight repression by a combination of the catabolite repressor glucose and the anti-inducer D-fucose, a non-metabolizable methylpentose (6-deoxygalactose) (28–30). For *atpB*, expression was controlled by the *lac* operator-controlled T7 promoter (*T7p-laco*). The T7 promoter is not recognized by *E. coli* RNA polymerases but needs a separate source coding for T7 RNA polymerase (31), which is provided by plasmid-encoded expres-

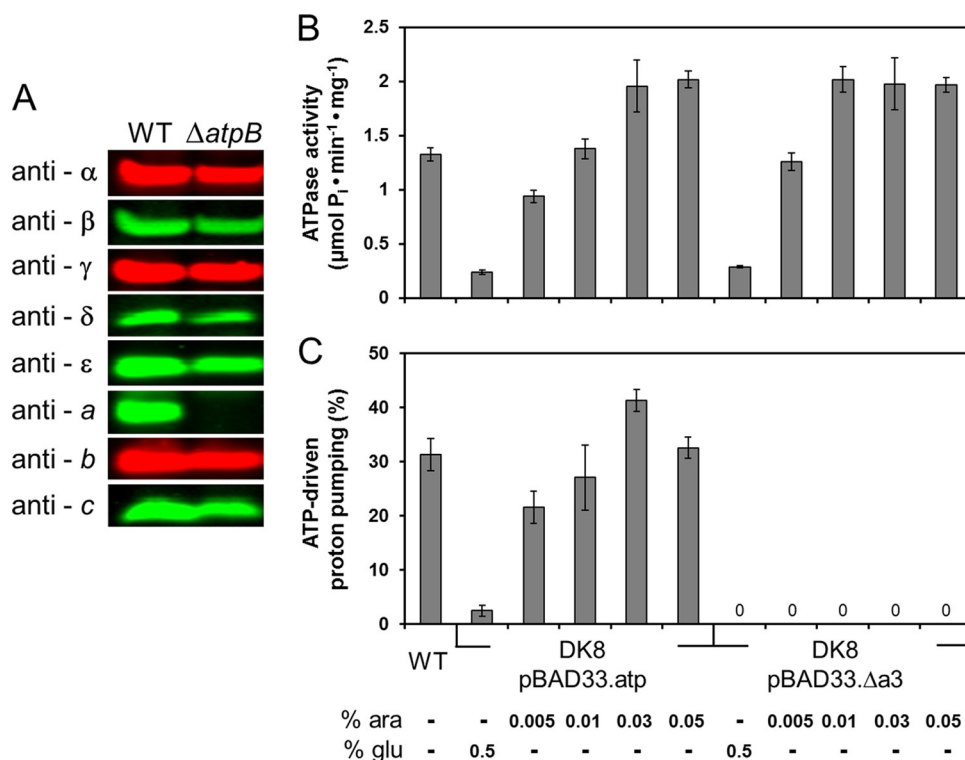


**FIG 1** Characterization of the F<sub>0</sub>F<sub>1</sub>-*a* subcomplex. (A) Cells of *E. coli* DK8 transformed with pBWU13 (WT) or pJGA1 ( $\Delta atpB$ ) were grown in LB medium with ampicillin and harvested at OD = 0.8 to 1.0. After resuspension in sample loading buffer, cells were incubated for 5 min at 99°C. The amount of cell extract applied per lane (20  $\mu\text{g}$ ) was calculated according to the determination of Neidhardt et al. (38) that 160  $\mu\text{g}$  of protein was present per ml cell culture at OD = 1.0. Immunolabeling was performed using mouse (anti- $\beta$ , anti- $\delta$ , anti- $\epsilon$ ) or rabbit (anti- $\alpha$ , anti- $\gamma$ , anti-*b*) polyclonal antisera or mouse monoclonal antibodies (anti-*a*, anti-*c*) raised against the individual subunits of the ATP synthase. (B and C) ATP hydrolysis (B) and ATP-driven proton-pumping activity (C) of membrane vesicles of DK8/pBAD33.atp and DK8/pBAD33. $\Delta a3$ , respectively, determined using the WT as a control. Cells were grown in LB medium with chloramphenicol in the presence of different arabinose concentrations for induction of the *araBADp* expression system or in the presence of glucose for repression as indicated. Cells were harvested at OD = 0.8 to 1.0, and inverted membrane vesicles were prepared. ATP-driven proton translocation was measured via ACMA fluorescence quenching. The relative magnitudes of quenching induced by addition of ATP are shown. ara, arabinose; glu, glucose.

sion of T7 *gene1* under the control of the *lac* operator-controlled T5N25 promoter (51). To guarantee complete repression of the IPTG-inducible promoters, lactose present in LB medium was removed. In addition, the start codon of the *atpB* gene present under the control of T7*p-laco* was exchanged from ATG to GTG in order to prevent the synthesis of subunit *a* under noninduced conditions (see below).

Figure 2 shows the configuration of the test system and its different states during cell growth. The *atp* deletion strain DK8 was transformed with three different plasmids bearing different resistance cassettes and origins to generate compatibility within one cell: (i) a pBAD33 derivative (p15A *ori*; Cm<sup>r</sup>) carrying the structural genes of the *atp* operon with a deletion of the *atpB* gene (*atpEFHAGDC*) under the control of *araBADp*, (ii) a pET-22b derivative (pMB1 *ori*; Ap<sup>r</sup>) encoding the *atpB* gene under the control of the IPTG-inducible T7-*laco* promoter, and (iii) a pSC101 derivative (Kan<sup>r</sup>) containing *gene1* of phage T7, which codes for the T7 promoter-specific RNA polymerase, present under the control of the IPTG-inducible promoter T5N25-*laco*. The cartoon illustrates the induction or repression states of the different promoters present. As shown in the left panel, after addition of arabinose to cells inoculated at an OD of 0.05, *araBADp* was induced and allowed expression of the *atpEFHAGDC* genes such that all F<sub>0</sub>F<sub>1</sub> subunits except subunit *a* (F<sub>0</sub>F<sub>1</sub>-*a*) were synthesized. Due to the absence

of IPTG and further precautions, the *lac* operator-controlled promoters were completely repressed. As shown in the middle panel, at OD = 0.3, *araBADp* was repressed by the simultaneous addition of glucose and D-fucose, thereby stopping the transcription of *atpEFHAGDC*; furthermore, after incubation for 30 min, the *atp* mRNA present within the cell was completely degraded as indicated by real-time RT-PCR results (see below). Due to this time delay, the *de novo* biosynthesis of F<sub>0</sub>F<sub>1</sub> subunits and, therefore, the formation of new F<sub>0</sub>F<sub>1</sub>-*a* complexes as well were completely prevented. As shown in the right panel, the delayed induction of the *lac* operator-controlled T7 and T5N25 promoters with IPTG then enabled the individual synthesis of subunit *a*, which can be integrated only into preformed partially assembled F<sub>0</sub>F<sub>1</sub>-*a* complexes present within the cytoplasmic membrane (referred to as F<sub>0</sub>F<sub>1</sub>-*a* + *a*). To control the synthesis of F<sub>0</sub>F<sub>1</sub> subunits, subunit *b* as a representative for F<sub>0</sub>F<sub>1</sub>-*a* and subunit *a* itself were detected by immunoblotting. The formation of a functionally assembled F<sub>0</sub>F<sub>1</sub> complex is controlled by assaying DCCD-sensitive ATPase activity and ATP-driven proton translocation as well as ATP synthesis. To facilitate reading, DK8/pBWU13 (*atpBEF-HAGDC*, the expression system usually applied for studies of *E. coli* ATP synthase [10, 40]) is always referred to here as WT, whereas DK8 transformed with pBAD33.atp, containing the structural wild-type *atp* genes, as well as plasmids pET-22b and pT7POL26, is termed F<sub>0</sub>F<sub>1</sub>. F<sub>0</sub>F<sub>1</sub> contains plasmids pET-22b and pT7POL26 in addition,

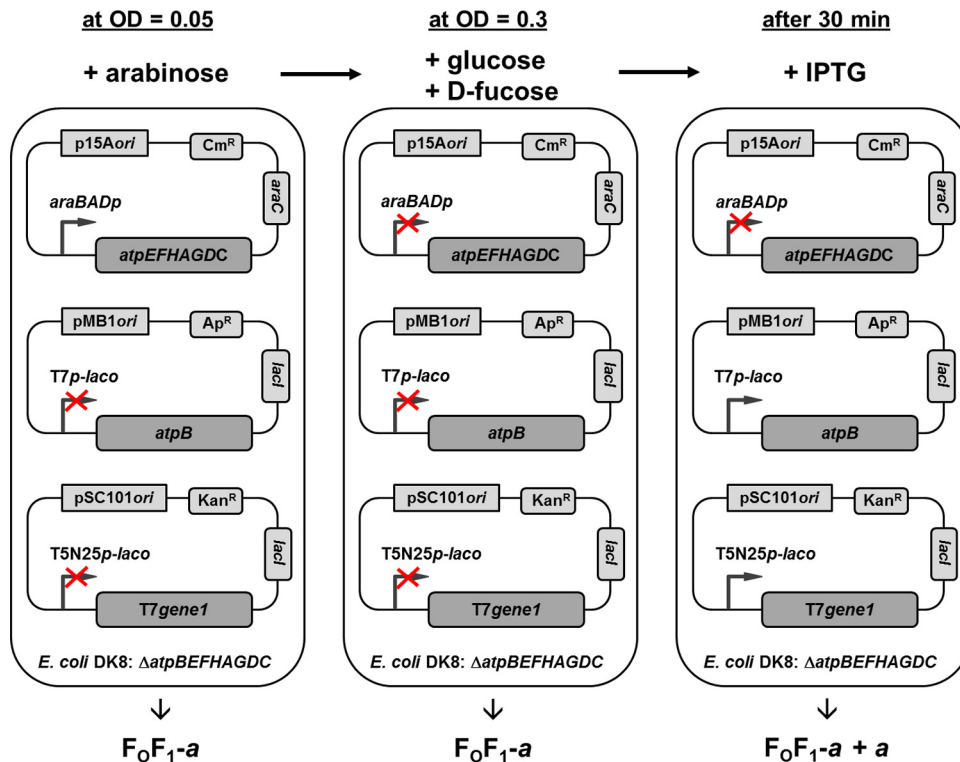


FIG 2 *In vivo* system for time-delayed assembly of membrane-integrated subunit *a* into preformed  $F_0F_1$ -*a*. A detailed description is given in the text.

in order to facilitate resemblance of the corresponding subsequent expression of  $F_0F_1$ -*a* by use of pBAD33.Δa3, pET22-*atpB*(-GTG), and pT7POL26.

**Tightly regulated expression of *atpB*.** DK8 transformed only with pBAD33.Δa3 was not capable of ATP-driven proton translocation (Fig. 1C). However, in  $F_0F_1$ -*a*, in which plasmids pET22-*atpB* and pT7POL26 are also present, a signal comparable to that seen with the WT was observed (Fig. 3A), indicating that the *lac*-controlled promoters T7 and T5N25 were not completely repressed. To gain complete repression, in a first step, the LB medium used for growth was preincubated with β-Gal to remove residual lactose molecules (Fig. 3A) known to be present in various amounts in yeast extracts used for preparation of LB medium (37). With increasing amounts of β-Gal (up to 10 U/ml LB medium), a significant reduction of levels of subunit *a* present in membrane vesicles as well as a reduction of ATP-driven proton translocation could already be observed. However, the fluorescence quenching of  $F_0F_1$ -*a* in the absence of IPTG (see Fig. 3A; see also Fig. S1 in the supplemental material) revealed that complete repression could not be obtained. In a second step, the ATG start codon of *atpB* was exchanged to the weaker start codon GTG or TTG to reduce in general the synthesis of subunit *a*. In both cases, a further reduction in synthesis of subunit *a*, as well as of the ATP-driven proton translocation, could be observed (Fig. 3B; see also Fig. 6). Therefore, the following experiments were performed with preincubation of LB medium with β-Gal and the start codon of *atpB* being changed to GTG. For induction of *lac*-controlled promoters, an IPTG concentration of 0.1 mM was determined, allowing a synthesis rate of subunit *a* comparable to that seen with the WT or  $F_0F_1$  as revealed by immunoblotting with anti-*a* anti-

bodies as well as by ACMA fluorescence quenching (Fig. 3B; see also Fig. S1 in the supplemental material).

**Tightly regulated expression of *atpEFHAGDC*.** During glucose repression in LB medium, neither target protein nor ACMA fluorescence quenching could be observed, whereas with increasing concentrations of arabinose (up to 0.03% [wt/vol]), the ATP-driven proton translocation as well as the presence of subunits *a* and *b* increased to values comparable to those seen with the WT (see Fig. S2 in the supplemental material).

The centerpiece of the *in vivo* assembly system is the time-delayed synthesis of subunit *a* to allow its integration into preformed  $F_0F_1$ -*a* subcomplexes. To prevent simultaneous *de novo* biosynthesis of  $F_0F_1$ , the complete degradation of the *atpEFHAGDC* mRNA prior to induction of *atpB* expression by IPTG is a prerequisite. The level of *atp* mRNA was measured by real-time RT-PCR using sequence-specific primer pairs *atpE'F* (1 and 2) and *atpA* (3 and 4) annealing in different genes of the *atp* operon. To verify the specific annealing of the primers, total RNA of the plasmid-free *atp* deletion strain DK8 was used as a control (data not shown).

For a complete repression of the *araBADp* expression system,  $F_0F_1$ -*a* was grown in the presence or absence of arabinose for induction (+ara) up to an OD of 0.3 before glucose or D-fucose or both (+glu + fuc or +glu/fuc) were added for another 30 min. Cells were harvested in the late exponential phase, and total RNA was purified for analysis of *atp* mRNA by real-time RT-PCR. For a complete repression of the *araBAD* promoter as well as of D-fucose as an anti-inducer was essential (Fig. 4). In the absence of arabinose, a background of *atp* mRNA within the range of 0% to 2% compared to

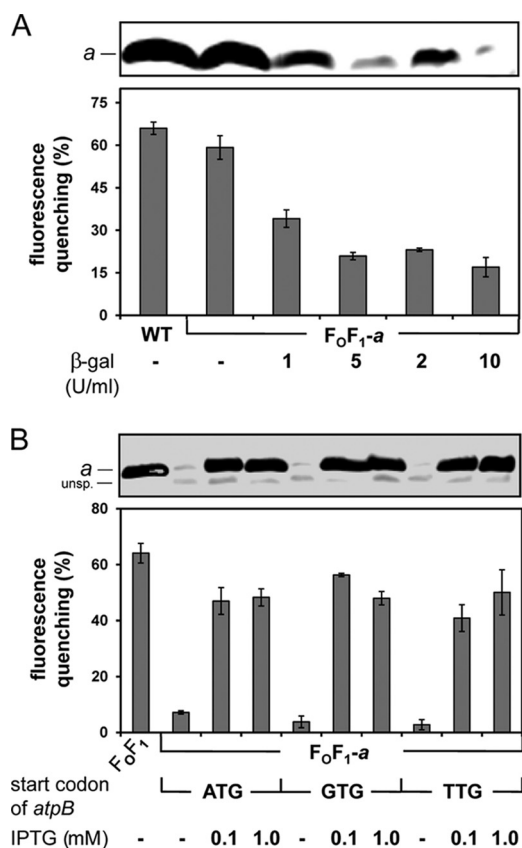


**FIG 3** T7p-lacO-driven expression of *atpB*. (A)  $\beta$ -Gal incubation for removal of lactose present in LB medium. DK8 transformed with pBWU13 (WT, control) or with pBAD33. $\Delta$ a3, pET22-atpB, and pT7POL26 (F<sub>0</sub>F<sub>1</sub>-a) was grown in LB medium supplemented with antibiotics and, in the case of F<sub>0</sub>F<sub>1</sub>-a, with 0.03% arabinose for induction of *araBADp*-controlled *atpEFHAGDC* expression. Prior to cell growth, the LB medium was incubated overnight with  $\beta$ -Gal concentrations as indicated. (B) Variation of the IPTG concentration and the start codon of T7 promoter-controlled *atpB*. DK8 transformed with pBAD33.atp, pET-22b, pT7POL26 (F<sub>0</sub>F<sub>1</sub>), pBAD33. $\Delta$ a3, pET22-atpB, pT7POL26 (F<sub>0</sub>F<sub>1</sub>-a; ATG), pBAD33. $\Delta$ a3, pET22-atpB-GTG, pT7POL26 (F<sub>0</sub>F<sub>1</sub>-a; GTG), or pBAD33. $\Delta$ a3, pET22-atpB-TTG, pT7POL26 (F<sub>0</sub>F<sub>1</sub>-a; TTG) was grown in  $\beta$ -Gal-preincubated LB medium supplemented with antibiotics, 0.03% arabinose, and IPTG as indicated. Cells were harvested at OD = 0.8 to 1.0 and membrane vesicles prepared. Upper panels, immunoblot analysis of membrane vesicles (20  $\mu$ g/lane). Immunolabeling was performed using monoclonal mouse anti-*a* antibodies. Lower panels, ATP-driven proton translocation of membrane vesicles measured via ACMA fluorescence quenching. The relative magnitudes of quenching induced by the addition of ATP are shown. unsp., unspecific immunolabeling.

the level seen with the system fully induced by arabinose could be observed in the presence of glucose or D-fucose or of both repressors (Fig. 4A). Nevertheless, under these conditions, ATP-driven proton translocation could not be observed (see Fig. S2 in the supplemental material), indicating that the amount of F<sub>0</sub>F<sub>1</sub> subunits synthesized was extremely small. However, in the presence of arabinose, a comparable repression of the *araBAD* promoter could be obtained only by simultaneous addition of glucose and D-fucose (Fig. 4). Glucose was added at the concentration usually applied for growth of cells in minimal medium with glucose as the sole carbon and energy source (0.5% [wt/vol]) to maintain the repressed status also during the residual growth phase in the time-delayed *in vivo* assembly experiments (degradation of *atp* mRNA

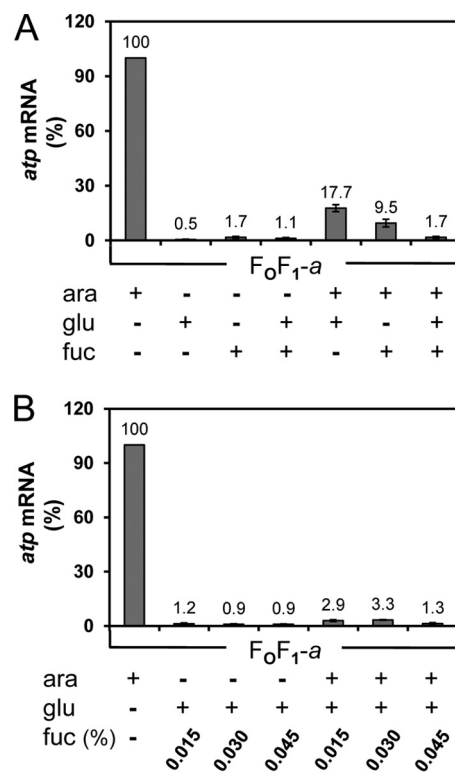


**FIG 4** Repression of *araBADp* by glucose/D-fucose determined by real-time RT-PCR. Cells were grown in  $\beta$ -Gal-preincubated LB medium supplemented with antibiotics in the presence (+) or absence (-) of arabinose as an inducer up to OD = 0.3 before glucose/D-fucose was added as indicated for another 30 min. Total RNA was isolated from DK8 bearing pBAD33. $\Delta$ a3, pET22-atpB-GTG, pT7POL26 (F<sub>0</sub>F<sub>1</sub>-a), and primer pair *atpE'F* (1 and 2) was applied for real-time RT-PCR. (A) Repression of the *araBADp* by glucose and D-fucose. (B) Determination of the D-fucose concentration necessary for repression. ara, arabinose; fuc, D-fucose; glu, glucose.

for 30 min and subsequent incubation with IPTG for 1 h), since glucose is metabolized in glycolysis. D-Fucose, a nonmetabolizable methylpentose (6-deoxygalactose), functions as a competitor to arabinose, resulting in a repression of *araBADp* when added in a slight molar excess over arabinose (52). In addition, IPTG is known to be an inhibitor of the *araBADp* expression system. Crosstalk between *araBADp* and *lac* operator-controlled promoters prevents them from being used simultaneously in the same cell (53). Under the time-delayed *in vivo* assembly conditions, this inhibitory effect of IPTG was advantageous, since the repression of the *araBAD* promoter was further strengthened.

To determine the time delay necessary for a complete degradation of the *atp* mRNA, cells were grown in the presence of arabinose at up to OD = 0.3 before glucose/D-fucose was added as described above. Total RNA was purified from samples taken after several time intervals after the addition of glucose/D-fucose. In F<sub>0</sub>F<sub>1</sub>, the *atp* mRNA was rapidly degraded, revealing a half-life for its stability of approximately 3 min as shown by real-time RT-PCR with primer pairs *atpE'F* and *atpA* (Fig. 5A), which correlates well with the half-life of *atpE* mRNA determined to be 5 to 6 min with independent methods (54).

A complete degradation of *atp* mRNA with a background level below 2% was always obtained within much less than 30 min (compare Fig. 5A to Fig. S3 in the supplemental material). In

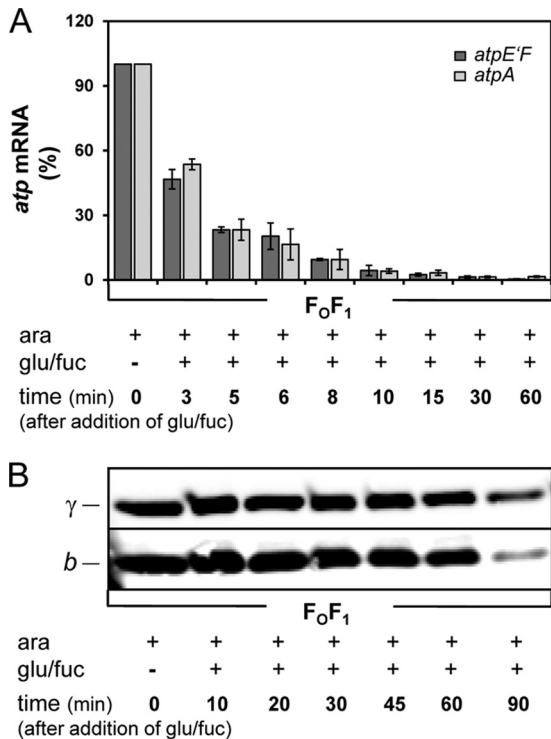


**FIG 5** Degradation of *atp* mRNA (A) and stability of  $F_0F_1$  (B) after repression of *araBADp* controlling expression of *atpEFHAGDC*. DK8 carrying plasmids pBAD33.*atp*, pET-22b, and pT7POL26 ( $F_0F_1$ ) was grown as described in the Fig. 4 legend. At each time point indicated, cells were harvested for isolation of RNA (A) or immunoblot analysis (B). (A) Real-time RT-PCR was performed using primer pairs *atpE'F* (1 and 2) (dark gray) and *atpA* (3 and 4) (light gray). (B) Cell lysates were prepared and applied as described in the Fig. 1 legend. For immunolabeling, monoclonal mouse anti-*b* and polyclonal rabbit anti- $\gamma$  antibodies were applied. ara, arabinose; fuc, D-fucose; glu, glucose.

addition, the degrees of degradation of *atp* mRNA were comparable in  $F_0F_1$  and  $F_0F_1$ -a as shown for primer pair *atpE'F* (Fig. S3), although, in general, the amount of *atp* mRNA present in  $F_0F_1$ -a under fully arabinose-induced conditions was always reduced compared to that present in  $F_0F_1$  (compare Fig. S3 in the supplemental material to Fig. 6A).

**Stability of  $F_0F_1$  under *araBADp*-repressed conditions.** Due to the time delay necessary for removal of *atp* mRNA as well as the incubation time with IPTG for expression of the missing subunit, the stability of the ATP synthase complexes present in the membrane had to be guaranteed at least for the next 90 min in order to allow a subsequent analysis of the functional status of the enzyme complexes. To study the stability of  $F_0F_1$ , cells were grown in the presence of arabinose to an OD = 0.3 before addition of glucose/D-fucose. Subsequently, samples were taken after several time intervals and the cell lysates analyzed by immunoblotting. For immunolabeling, antibodies against subunit *b* and  $\gamma$  were applied. As shown in Fig. 5B, both subunits were highly stable for at least 60 min after the addition of glucose/D-fucose. After 90 min, a reduction of both subunits could be observed, whereupon subunit *b* appeared to be more degraded as subunit  $\gamma$ . While the *b* dimer was exposed at the periphery of the enzyme complex, subunit  $\gamma$  was embedded within its center, shielded by the  $\alpha_3\beta_3$  hexamer, subunit  $\epsilon$ , and the  $c_{10}$  ring and, therefore, possibly more protected against proteolytic degradation. A comparison with Fig. 6B re-

vealed that the degradation rate of subunit *a*, which was also located at the periphery of  $F_0F_1$ , was comparable to that of subunit *b*. Nevertheless, the amount of  $F_0F_1$  still present in the membrane was sufficient to allow determination of its functional capabilities in ATP hydrolysis as well as ATP synthesis (compare Fig. 6C to E). A quantification using DCCD-sensitive ATPase activity revealed that approximately 30% of the enzyme complexes were still functional after 90 min of repression (compare Fig. 6C).

**Time-delayed *in vivo* assembly of subunit *a* into preformed  $F_0F_1$ -a.** After determination of all parameters necessary, the following test procedure was applied. LB medium preincubated overnight with 10 U/ml of  $\beta$ -Gal, supplemented with antibiotics as well as 0.03% arabinose, was inoculated to OD = 0.05 with  $F_0F_1$ -a. At OD = 0.3, 0.5% glucose and 0.045% D-fucose were added and, after complete degradation of *atpEFHAGDC* mRNA within 30 min, 0.1 mM IPTG was added for 1 h to enable time-delayed synthesis of subunit *a* (compare Fig. 2). Subsequently, cells were harvested, usually at an OD of about 1, total RNA as well as inverted membrane vesicles was prepared, and the activity of the ATP synthase was analyzed. As a control,  $F_0F_1$  samples were handled correspondingly except for the addition of IPTG. All in all, seven different cell batches were grown, each with the additives noted in Fig. 6 added at the time points indicated above.

Real-time RT-PCR revealed that under arabinose-induced conditions, *atp* mRNA was present within the cells, whereas in  $F_0F_1$ -a, the amount was slightly reduced compared to that seen with  $F_0F_1$  (Fig. 6A). In samples containing glucose/fucose, the *atp* mRNA had been completely degraded, revealing that *de novo* synthesis of  $F_0F_1$  subunits was no longer possible (Fig. 6A).

The immunoblot analysis showed a strong synthesis of subunit *b* under arabinose-induced conditions (Fig. 6B). After addition of glucose/D-fucose in the absence of arabinose, no subunit *b* could be detected in  $F_0F_1$ -a. Only in the case of  $F_0F_1$ , possibly due to the slightly increased stability of the *atp* mRNA, a small amount of subunit *b* could be detected, further promoted by the high avidity of the polyclonal antiserum with respect to its antigen. However, no subunit *a* could be observed in  $F_0F_1$  under these conditions. The samples first induced with arabinose and then repressed by glucose/D-fucose showed significant bands for subunits *a* and *b* in the case of  $F_0F_1$  and a comparable band for subunit *b* in the case of  $F_0F_1$ -a, thereby revealing that the enzyme (sub)complex was still present in membrane vesicles after 90 min. After addition of IPTG to  $F_0F_1$ -a, subunit *a* was slightly overproduced beyond its stoichiometric ratio. Nevertheless, all components necessary to allow the generation of a functional  $F_0F_1$  complex, namely,  $F_0F_1$ -a + *a*, were present within the cytoplasmic membrane.

Bacterial ATP synthases can function either as ATP synthase or as ATP hydrolase in a manner dependent on the physiological status of the cells. Therefore, the functionality of  $F_0F_1$ -a + *a* was analyzed with respect to its DCCD-sensitive ATPase activity, ATP-driven proton translocation, and ATP synthesis (Fig. 6C, D, and E, respectively). As expected, both  $F_0F_1$  and  $F_0F_1$ -a showed high levels of ATPase activities under arabinose-induced conditions. Under repressing conditions, only extremely low levels of ATPase activities could be observed in the case of  $F_0F_1$ , which correlates well with the amount of subunit *b* observed by immunoblotting. The ATPase activities observed in the samples, which were first induced with arabinose and then repressed with glucose/D-fucose, were also in good agreement with the immunoblot data and could, therefore, be used as a quantitative measure for protein

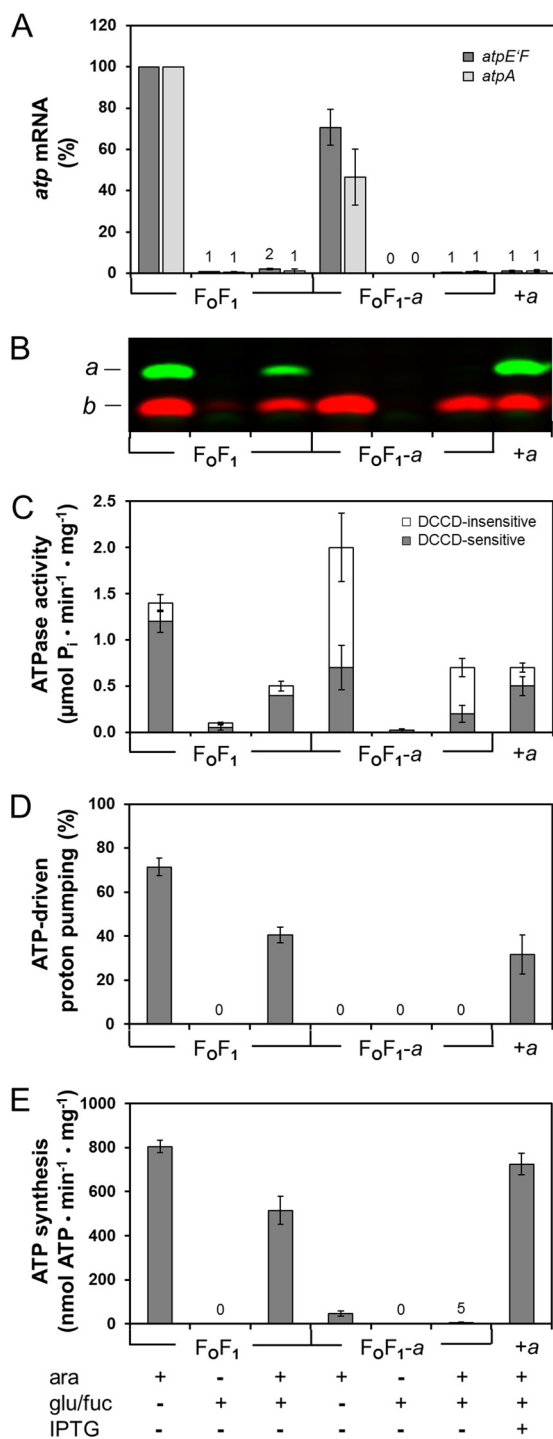


**FIG 6** *In vivo* assembly of subunit *a* into preformed F<sub>0</sub>F<sub>1</sub>-*a* complexes. DK8 carrying plasmid pBAD33.atp, pET-22b, pT7POL26 (F<sub>0</sub>F<sub>1</sub>), pBAD33.Δa3, pET22-atpB-GTG, or pT7POL26 (F<sub>0</sub>F<sub>1</sub>-*a*) was grown in LB medium preincubated with β-Gal in the presence of antibiotics. Seven independent cell batches were prepared in parallel containing the additives as indicated. +ara or +glu/fuc, the addition of inducer or repressor, respectively, occurred directly after inoculation of the medium. +ara +glu/fuc, cells were grown in the presence of arabinose up to OD = 0.3 before addition of glucose/D-fucose. In the case of F<sub>0</sub>F<sub>1</sub>-*a* + *a*, 0.1 mM IPTG was added subsequently for 1 h as described in Materials and Methods. All cells were harvested at the same time, membrane vesicles were prepared, and a small volume of cell culture was used for isolation of total RNA. (A) Level of *atp* mRNA. The amount of *atp* mRNA was determined via real-time RT-PCR using primer pairs *atpE'F* (1 and

stability. The results indicate that for F<sub>0</sub>F<sub>1</sub> as well as for F<sub>0</sub>F<sub>1</sub>-*a*, about one-third of the enzyme complexes were still present in the membranes after repression for 90 min. ATPase activities of membrane vesicles were measured with or without pretreatment by DCCD. DCCD is known to label specifically the carboxyl group of cD61, thereby blocking the rotation of the subunit *c* ring and the proton translocation. Due to the inhibition of the rotation by DCCD, ATP hydrolysis cannot occur in coupled F<sub>0</sub>F<sub>1</sub> complexes and, therefore, ATP hydrolysis is inhibited. Whereas the DCCD sensitivity of the ATPase activity was 80% to 85% in F<sub>0</sub>F<sub>1</sub>, a value usually observed in membrane vesicles (46, 55), F<sub>0</sub>F<sub>1</sub>-*a* showed comparably low sensitivity toward DCCD (Fig. 6C). In the sample synthesizing F<sub>0</sub>F<sub>1</sub>-*a* + *a*, the ATPase activity was comparable to F<sub>0</sub>F<sub>1</sub>-*a* activity, as expected; however, the DCCD sensitivity was increased from 29% to 71%. This indicates a functional incorporation of subunit *a* into F<sub>0</sub>F<sub>1</sub>.

In the next step, ATP-driven proton translocation was tested (Fig. 6D). Proton translocation into membrane vesicles was monitored by acidification of the lumen leading to fluorescence quenching of the pH-sensitive dye ACMA. Membranes containing F<sub>0</sub>F<sub>1</sub> under arabinose-induced conditions generated a fluorescence quenching of 71%, whereas under repressed conditions no proton pumping could be observed. In the sample first induced by arabinose and then repressed by glucose/D-fucose, F<sub>0</sub>F<sub>1</sub> produced a fluorescence quenching of 41%, with only one-third of F<sub>0</sub>F<sub>1</sub> present in the membrane (compare Fig. 6C). In general, the quenching of ACMA fluorescence by proton gradients is known to be nonquantitative, so the ratios need not correspond exactly. In the case of ATP-driven proton pumping, results depend on the amount of F<sub>0</sub>F<sub>1</sub> present in the membrane as well as on the proton permeability of the membrane itself (in this context, compare references 40 and 56). In the case of membranes containing F<sub>0</sub>F<sub>1</sub>-*a*, no ACMA fluorescence quenching could be detected in the absence of subunit *a*. To verify the functionality of inverted membrane vesicles, proton translocation through the respiratory chain energized by oxidation of NADH was monitored. NADH-driven proton translocation with and without pretreatment by DCCD was measured and revealed fluorescence quenching of 70% to 80% in both cases (data not shown). The protons pumped into the vesicles were retained in the lumen, thereby showing that F<sub>0</sub>F<sub>1</sub>-*a* does not increase proton leakage of the vesicle membrane. In contrast, membranes with F<sub>0</sub>F<sub>1</sub>-*a* + *a* showed ATP-driven proton translocation with a fluorescence quenching of 32%, again supporting the idea of functional assembly of subunit *a* into preformed F<sub>0</sub>F<sub>1</sub>-*a* complexes. Furthermore, F<sub>0</sub>F<sub>1</sub>-*a* + *a* restored proton translocation activity to the value observed for F<sub>0</sub>F<sub>1</sub>. For

2) (dark gray) and *atpA* (3 and 4) (light gray). The amount of *atp* mRNA present in the samples grown with arabinose was set to 100% for F<sub>0</sub>F<sub>1</sub>. (B) Immunoblot analysis of membrane vesicles (20 μg protein/lane). Immunolabeling was performed using monoclonal mouse anti-*a* (green) or polyclonal rabbit anti-*b* (red) antibodies. (C) ATPase activity of membrane vesicles. The gray and white portions of the bars represent the DCCD-sensitive and DCCD-insensitive fractions of ATP hydrolysis, respectively. (D) ATP-driven proton translocation of membrane vesicles measured by ACMA fluorescence quenching. The relative magnitudes of quenching induced by the addition of ATP are shown. (E) ATP synthesis of membrane vesicles driven by NADH oxidation. The amount of ATP synthesized after addition of NADH was determined luminometrically with a luciferin/firefly luciferase system and corrected for nonspecific background activity. Experimental details are described in Materials and Methods. ara, arabinose; fuc, D-fucose; glu, glucose.

$F_0F_1-a + a$  as well as  $F_0F_1$ , the proton-translocating activity was completely abolished after preincubation of the membranes with DCCD (data not shown).

For the synthesis of ATP, the proton motive force was generated by the respiratory chain upon oxidation of NADH (Fig. 6E). Under normal growth conditions, the ATP synthase is mainly used as an ATP-generating machine instead of hydrolyzing ATP to generate a proton motive force. Therefore, it is essential to verify that the assembly of subunit *a* into preformed  $F_0F_1-a$  complexes yielded an enzyme also functional in this aspect. Membrane vesicles containing  $F_0F_1-a + a$  exhibited ATP synthesis with a 90% yield compared to membranes with  $F_0F_1$ . This clearly demonstrates the presence of  $F_0F_1$  complexes with tightly coupled proton translocation in  $F_0$  and catalysis in  $F_1$ . At first glance, the ATP synthesis rate obtained seems to be unusually high compared to the amount of functional  $F_0F_1$  present in the membrane. However, the rate of ATP synthesis by the ATP synthase is generally limited by the rate of energy production via the respiratory chain in membrane vesicles, as has been shown by fractional inactivation of  $F_0F_1$  with DCCD (57). Under these conditions, the rate of ATP synthesis per mol of  $F_0F_1$  remaining active in the membrane is increased, using the ATP hydrolysis rates as the defining parameter for calculation of active ATP synthase complexes (57). In summary, all results obtained are consistent and demonstrate a functional time-delayed *in vivo* assembly of subunit *a* into preformed  $F_0F_1-a$  complexes.

## DISCUSSION

**Time-delayed *in vivo* assembly.** In the present work, a general approach to study the assembly of membrane-integrated as well as soluble heteromultimeric protein complexes *in vivo* has been established by the use of two independent expression systems as described in Results. Due to the time-delayed synthesis of at least one of the subunits, partially assembled complexes can be generated and studied with respect to stability and functionality and the missing subunit(s) subsequently synthesized and possibly integrated to obtain a functional enzyme complex. As an ideal tool to determine the essential parameters, the assembly of the membrane-integrated subunit *a* into preformed  $F_0F_1-a$  subcomplexes has been chosen due to the known stability of this subcomplex (23, 24, 68). Furthermore, the *in vivo* assembly system has already successfully been transferred to a  $F_0F_1-\delta$  construct. A functional  $F_0F_1$  complex could be assembled after time-delayed synthesis of missing subunit  $\delta$ , thereby indicating that under these conditions also, the conformation of the preformed subcomplexes  $ab_2$  and  $c_{10}\alpha_3\beta_3\gamma\epsilon$ , present in the membrane, remained in a ready-to-use state (68).

***In vivo* versus cell-free protein synthesis.** A major advantage of an *in vivo* system is the possibility to enable a sequential synthesis of proteins without any further manipulation. Recently, approaches involving cell-free protein synthesis have emerged as a promising tool for the study of membrane protein complexes, including the ATP synthase (24, 58, 59). However, in order to obtain sequential protein synthesis, a purification step of the partially assembled protein complex or at least of membrane vesicles has to be included, which is then followed by cell-free protein synthesis as described in detail by Kuruma et al. (24). In that approach, *E. coli* membrane vesicles or liposomes containing *Bacillus* PS3  $F_0F_1-a$  subcomplexes were isolated or generated and, in a subsequent second step, applied to the cell-free PURE system in

order to generate functional  $F_0F_1$  by *in vitro* cell-free synthesis of subunit *a* (24), a procedure yielding results similar to those described in the text. However, under such conditions, the stability of the partially assembled subcomplex(es) is a prerequisite to allow for purification and subsequent reconstitution or for manipulation of cells by sonication, high pressure, and centrifugation, which is at hand in the case of  $F_0F_1-a$ , but not a general feature of partially assembled subcomplexes.

**ATPase activity of partially assembled  $F_0F_1-a$ .** The presence of ATP hydrolysis in  $F_0F_1-a$ , at rates similar to those seen with wild-type  $F_0F_1$ , strengthens the view that comparable conformations at least of the catalytically active, membrane-bound core complex composed of  $c_{10}\alpha_3\beta_3\gamma\epsilon$  are maintained in the two complexes. Whereas ATPase activities of *E. coli*  $F_0F_1-a$  have been determined in inverted membrane vesicles in a manner independent of their plasmid- or chromosome-based expression (compare reference 6), no ATPase activities could be observed for *Bacillus* PS3  $F_0F_1-a$  (23). However, in the latter case, the  $F_0F_1-a$  complex had been solubilized from *E. coli* membranes, purified by affinity chromatography via His-tagged subunit  $\beta$ , and reconstituted into liposomes prior to ATPase activity measurements. Although a stable complex can be isolated under these conditions, the removal of the complex from its natural membrane environment might change the conformation or positioning of one or some of the partially assembled  $F_0F_1$  subunits, thereby possibly inhibiting ATPase activity. Nevertheless, this process can be reversed by addition of subunit *a* (23). However, a putative function of the *b* dimer as an anchor rail to prevent the rotation of the  $c_{10}$  ring in the absence of subunit *a*, thereby inhibiting the ATPase activity of the partially assembled  $F_0F_1$  complexes as proposed by Ono et al. (23), can be excluded for the ATP synthase of *E. coli*.

In  $F_0F_1$ , ATP hydrolysis in  $F_1$  is tightly coupled to proton translocation in  $F_0$  and is, therefore, sensitive to DCCD inhibition. In the absence of subunit *a*, the two half-channels essential for proton translocation are missing and proton translocation across the cytoplasmic membrane is no longer possible. Therefore, with the common understanding of the rotary mechanism of the enzyme, the robust structure of  $F_0F_1-a$  as well as the observed ATPase activity implies that either the rotation of the central stalk (subunits  $\gamma$  and  $\epsilon$ ) is uncoupled from the subunit *c* oligomer or that the  $c_{10}$  ring remains coupled and corotates with subunits  $\gamma\epsilon$  during ATP hydrolysis, thereby supporting a free rotation without proton translocation of the rotor part of the enzyme ( $c_{10}\gamma\epsilon$ ) within the membrane. The latter interpretation could be favored, since free rotation without proton translocation has already been demonstrated for  $F_0F_1$  purified from a mutant in which *cD61* was exchanged to asparagine or glycine (60). Furthermore, the observed partial inhibition of the ATPase activity of  $F_0F_1-a$  by DCCD can be explained by sterical hindrance of the rotation due to the bulky structure of the hydrophobic carbodiimide but simultaneously indicates a tight coupling between  $F_1$  and the  $c_{10}$  ring in the membrane. In addition, it implies that the carboxyl groups of *cD61* are in a protonated state at least in some of the *c* subunits, since binding of carbodiimides requires protonation as a prerequisite (61). Furthermore, the data support the view that no appreciable contact sites between the rotor and stator, namely,  $b_2$  and  $c_{10}$ , are present in the  $F_0$  part in the absence of subunit *a*.

**Subunit *a*, the last subunit being assembled into  $F_0F_1$ ?** All of these observations clearly demonstrate that a controlled synthesis of subunit *a* as well as a tightly regulated interaction with the other

F<sub>0</sub>F<sub>1</sub> subunits is essential for the viability of the cell. Subunit *a* is a protein of high hydrophobicity, and overexpression of the *atpB* gene causes growth inhibition of *E. coli* cells associated with cell elongation and an altered septum structure (62) and has been shown to dissipate the electrical potential of the membrane, probably due to an improper insertion of subunit *a* into the membrane (63). To avoid cell toxicity resulting from the presence of subunit *a*, *in vivo* overexpression is prevented by a rather unstable *atpB* gene transcript (54, 64) and a translational frameshifting at an additional ribosome binding site within the *atpB* reading frame (65) and, furthermore, improperly membrane-inserted subunit *a* is rapidly degraded by the membrane protease FtsH (8, 9).

The successful time-delayed assembly of subunit *a* into preformed F<sub>0</sub>F<sub>1</sub>-*a* complexes *in vivo* supports the view that subunit *a* is the last subunit being integrated into the enzyme complex (23–25), thereby finally generating a functional ATP synthase. From an energetic point of view, it appears favorable that the formation of the proton-conducting unit by interaction of subunit *a* with the c<sub>10</sub> ring is the last step during assembly, ensuring that partially assembled subcomplexes do not result in proton leakage, which might be lethal for the cell. However, one has to keep in mind that the use of knockout or deletion mutants arrests the assembly pathway at a certain point to enable the investigation of intermediate states. Recent studies on F<sub>0</sub>F<sub>1</sub> missing subunit δ revealed that also subunit δ can be integrated as the last subunit to assemble F<sub>0</sub>F<sub>1</sub> from *ab*<sub>2</sub> and c<sub>10</sub>α<sub>3</sub>β<sub>3</sub>γε using the same experimental design, a contradiction only at first glance, as discussed in detail elsewhere (68). Furthermore, for yeast mitochondria, a modular assembly of the ATP synthase has also been demonstrated which includes subcomplex formation between subunit *a* and the peripheral stalk prior to its binding to an F<sub>0</sub>F<sub>1</sub> core complex consisting of F<sub>1</sub> and the *c* ring (18). Nevertheless, also under these conditions, the formation of the proton translocating unit is the last step in assembly.

## ACKNOWLEDGMENTS

This work was supported by a grant of the Deutsche Forschungsgemeinschaft (DE482/1-1).

We thank Brigitte Herkenhoff-Hesselmann for expert technical assistance, Jörg-Christian Greie and Karlheinz Altendorf for critical reading of the manuscript, Julia Garrelfs and Judit Sauerland for generating plasmids pJGA1 and pJS1, and Stanley D. Dunn (University of Western Ontario, London, Canada) for providing antibodies against subunit γ.

## REFERENCES

1. von Ballmoos C, Cook GM, Dimroth P. 2008. Unique rotary ATP synthase and its biological diversity. *Annu. Rev. Biophys.* 37:43–64.
2. von Ballmoos C, Wiedenmann A, Dimroth P. 2009. Essentials for ATP synthesis by F<sub>1</sub>F<sub>0</sub> ATP synthases. *Annu. Rev. Biochem.* 78:649–672.
3. Kol S, Majczak W, Heerlien R, van der Berg JP, Nouwen N, Driessen AJM. 2009. Subunit *a* of the F<sub>1</sub>F<sub>0</sub> ATP synthase requires YidC and SecYEG for membrane insertion. *J. Mol. Biol.* 390:893–901.
4. Yi L, Jiang F, Chen M, Cain BD, Bolhuis A, Dalbey RE. 2003. YidC is strictly required for membrane insertion of subunits *a* and *c* of the F<sub>1</sub>F<sub>0</sub> ATP synthase and SecE of the SecYEG translocase. *Biochemistry* 42:10537–10544.
5. Yi L, Celebi N, Chen M, Dalbey RE. 2004. Sec/SRP requirements and energetics of membrane insertion of subunits *a*, *b*, and *c* of the *Escherichia coli* F<sub>1</sub>F<sub>0</sub> ATP synthase. *J. Biol. Chem.* 279:39260–39267.
6. Hermolin J, Fillingame RH. 1995. Assembly of F<sub>0</sub> sector of *Escherichia coli* H<sup>+</sup> ATP synthase. Interdependence of subunit insertion into the membrane. *J. Biol. Chem.* 270:2815–2817.
7. Pierson HE, Uhlemann EME, Dmitriev OY. 2011. Interaction with monomeric subunit *c* drives insertion of ATP synthase subunit *a* into the membrane and primes *a-c* complex formation. *J. Biol. Chem.* 286:38583–38591.
8. Akiyama Y, Ito K. 2003. Reconstitution of membrane proteolysis by FtsH. *J. Biol. Chem.* 278:18146–18153.
9. Akiyama Y, Kihara A, Ito K. 1996. Subunit *a* of proton ATPase F<sub>0</sub> sector is a substrate of the FtsH protease in *Escherichia coli*. *FEBS Lett.* 399:26–28.
10. Ballhausen B, Altendorf K, Deckers-Hebestreit G. 2009. Constant c<sub>10</sub> ring stoichiometry in the *Escherichia coli* ATP synthase analyzed by cross-linking. *J. Bacteriol.* 191:2400–2404.
11. Suzuki T, Ozaki Y, Sone N, Feniouk BA, Yoshida M. 2007. The product of *uncI* gene in F<sub>1</sub>F<sub>0</sub>-ATP synthase operon plays a chaperone-like role to assist *c*-ring assembly. *Proc. Natl. Acad. Sci. U. S. A.* 104:20776–20781.
12. Ozaki Y, Suzuki T, Kuruma Y, Ueda T, Yoshida M. 2008. UncI protein can mediate ring-assembly of *c*-subunits of F<sub>0</sub>F<sub>1</sub>-ATP synthase *in vitro*. *Biochem. Biophys. Res. Commun.* 367:663–666.
13. Brandt K, Müller DB, Hoffmann J, Hübert C, Brutschy B, Deckers-Hebestreit G, Müller V. 2013. Functional production of the Na<sup>+</sup> F<sub>1</sub>F<sub>0</sub> ATP synthase from *Acetobacterium woodii* in *Escherichia coli* requires the native AtpI. *J. Bioenerg. Biomembr.* 45:15–23.
14. Schneppe B, Deckers-Hebestreit G, Altendorf K. 1990. Overproduction and purification of the *uncI* gene product of the ATP synthase of *Escherichia coli*. *J. Biol. Chem.* 265:389–395.
15. Schneppe B, Deckers-Hebestreit G, Altendorf K. 1991. Detection and localization of the *i* protein in *Escherichia coli* cells using antibodies. *FEBS Lett.* 292:145–147.
16. Gay NJ. 1984. Construction and characterization of an *Escherichia coli* strain with a *uncI* mutation. *J. Bacteriol.* 158:820–825.
17. Liu J, Hicks DB, Krulwich TA. 2013. Roles of AtpI and two YidC-type proteins from alkaliphilic *Bacillus pseudofirmus* OF4 in ATP synthase assembly and nonfermentative growth. *J. Bacteriol.* 195:220–230.
18. Rak M, Gokova S, Tzagoloff A. 2011. Modular assembly of yeast mitochondrial ATP synthase. *EMBO J.* 30:920–930.
19. Kucharczyk R, Zick M, Bietenhader M, Rak M, Couplan E, Blondel M, Caubet S-D, di Rago J-P. 2009. Mitochondrial ATP synthase disorders: molecular mechanisms and the quest for curative therapeutic approaches. *Biochim. Biophys. Acta* 1793:186–199.
20. Koebmann BJ, Westerhoff HV, Snoep JL, Nilsson D, Jensen PR. 2002. The glycolytic flux in *Escherichia coli* is controlled by the demand for ATP. *J. Bacteriol.* 184:3909–3916.
21. al-Shawi MK, Parsonage D, Senior AE. 1990. Adenosine triphosphatase and nucleotide binding activity of isolated β-subunit preparations from *Escherichia coli* F<sub>1</sub>F<sub>0</sub>-ATP synthase. *J. Biol. Chem.* 265:5595–5601.
22. Senior AE, Muharemagić A, Wilke-Mounts S. 2006. Assembly of the stator in *Escherichia coli* ATP synthase. Complexation of α subunit with other F<sub>1</sub> subunits is prerequisite for δ subunit binding to the N-terminal region of α. *Biochemistry* 45:15893–15902.
23. Ono S, Sone N, Yoshida M, Suzuki T. 2004. ATP synthase that lacks F<sub>0</sub>*a*-subunit. Isolation, properties, and indication of F<sub>0</sub>*b*<sub>2</sub>-subunits as an anchor rail of a rotating *c*-ring. *J. Biol. Chem.* 279:33409–33412.
24. Kuruma Y, Suzuki T, Ono S, Yoshida M, Ueda T. 2012. Functional analysis of membranous F<sub>0</sub>-*a* subunit of F<sub>1</sub>F<sub>0</sub>-ATP synthase by *in vitro* protein synthesis. *Biochem. J.* 442:631–638.
25. Wittig I, Meyer B, Heide H, Steger M, Bleier L, Wumaier Z, Karas M, Schagger H. 2010. Assembly and oligomerization of human ATP synthase lacking mitochondrial subunits *a* and A6L. *Biochim. Biophys. Acta* 1797:1004–1011.
26. Ludlam A, Brunzelle J, Pribyl T, Xu X, Gatti DL, Ackerman SH. 2009. Chaperones of F<sub>1</sub>-ATPase. *J. Biol. Chem.* 284:17138–17146.
27. Straffon AFL, Prescott M, Nagley P, Devenish RJ. 1998. The assembly of yeast mitochondrial ATP synthase: subunit depletion *in vivo* suggests ordered assembly of the stalk subunits *b*, OSCP and *d*. *Biochim. Biophys. Acta* 1371:157–162.
28. Cagnon C, Valverde V, Masson J-M. 1991. A new family of sugar-inducible expression vectors for *Escherichia coli*. *Protein Eng.* 4:843–847.
29. Guzman LM, Belin D, Carson MJ, Beckwith J. 1995. Tight regulation, modulation, and high-level expression by vectors containing the arabinose P<sub>BAD</sub> promoter. *J. Bacteriol.* 177:4121–4130.
30. Beverin S, Sheppard DE, Park SS. 1971. D-Fucose as a gratuitous inducer of the L-arabinose operon in strains of *Escherichia coli* B/r mutant in gene *araC*. *J. Bacteriol.* 107:79–86.
31. Studier FW, Rosenberg AH, Dunn JJ, Dubendorff JW. 1990. Use of T7 RNA polymerase to direct expression of cloned genes. *Methods Enzymol.* 185:60–89.

32. Nielsen J, Hansen FG, Hoppe J, Friedl P, von Meyenburg K. 1981. The nucleotide sequence of the *atp* genes coding for the F<sub>O</sub> subunits *a*, *b*, *c* and the F<sub>1</sub> subunit *δ* of the membrane-bound ATP synthase of *Escherichia coli*. *Mol. Gen. Genet.* 184:33–39.
33. Kuo PH, Ketchum CJ, Nakamoto RK. 1998. Stability and functionality of cysteine-less F<sub>O</sub>F<sub>1</sub> ATP synthase from *Escherichia coli*. *FEBS Lett.* 426:217–220.
34. Noji H, Häsler K, Junge W, Kinoshita K, Jr, Yoshida M, Engelbrecht S. 1999. Rotation of *Escherichia coli* F<sub>1</sub>-ATPase. *Biochem. Biophys. Res. Commun.* 260:597–599.
35. Klionsky DJ, Brusilow WSA, Simoni RD. 1984. In vivo evidence for the role of the  $\epsilon$  subunit as an inhibitor of the proton-translocating ATPase of *Escherichia coli*. *J. Bacteriol.* 160:1055–1060.
36. Sambrook J, Russell DW. 2001. Molecular cloning: a laboratory manual, 3rd ed. Cold Spring Harbor Laboratory, Cold Spring Harbor, NY.
37. TaKaRa. 2012. Single protein production system (SPP system). TaKaRa Bio Inc., Japan.
38. Neidhardt FC, Ingraham JL, Schaechter M. 1990. Physiology of the bacterial cell. A molecular approach. Sinauer Associates, Sunderland, MA.
39. Strahl H, Greie JC. 2008. The extremely halophilic archaeon *Halobacterium salinarum* R1 responds to potassium limitation by expression of the K<sup>+</sup>-transporting KdpFABC P-type ATPase and by a decrease in intracellular K<sup>+</sup>. *Extremophiles* 12:741–752.
40. Krebstakies T, Aldag I, Altendorf K, Greie JC, Deckers-Hebestreit G. 2008. The stoichiometry of subunit *c* of *Escherichia coli* ATP synthase is independent of its rate of synthesis. *Biochemistry* 47:6907–6916.
41. Douglas M, Finkelstein D, Butow RA. 1979. Analysis of products of mitochondrial protein synthesis in yeast: genetic and biochemical aspects. *Methods Enzymol.* 56:58–66.
42. Schagger H, von Jagow G. 1987. Tricine-sodium dodecyl sulfate-polyacrylamide gel electrophoresis for the separation of proteins in the range from 1 to 100 kDa. *Anal. Biochem.* 166:368–379.
43. Birkenhäger R, Greie JC, Altendorf K, Deckers-Hebestreit G. 1999. F<sub>O</sub> complex of the *Escherichia coli* ATP synthase. Not all monomers of the subunit *c* oligomer are involved in F<sub>1</sub> interaction. *Eur. J. Biochem.* 264:385–396.
44. Dunn SD. 1986. Removal of the  $\epsilon$  subunit from *Escherichia coli* F<sub>1</sub>-ATPase using monoclonal anti- $\epsilon$  antibody affinity chromatography. *Anal. Biochem.* 159:35–42.
45. Stalz WD, Greie JC, Deckers-Hebestreit G, Altendorf K. 2003. Direct interaction of subunits *a* and *b* of the F<sub>O</sub> complex of *Escherichia coli* ATP synthase by forming an *ab*<sub>2</sub> subcomplex. *J. Biol. Chem.* 278:27068–27071.
46. Deckers-Hebestreit G, Simoni RD, Altendorf K. 1992. Influence of subunit-specific antibodies on the activity of the F<sub>O</sub> complex of the ATP synthase of *Escherichia coli*. I Effects of subunit *b*-specific polyclonal antibodies. *J. Biol. Chem.* 267:12364–12369.
47. Langemeyer L, Engelbrecht S. 2007. Essential arginine in subunit *a* and aspartate in subunit *c* of F<sub>O</sub>F<sub>1</sub> ATP synthase: effect of repositioning within helix 4 of subunit *a* and helix 2 of subunit *c*. *Biochim. Biophys. Acta* 1767:998–1005.
48. Vik SB, Simoni RD. 1987. F<sub>1</sub>F<sub>O</sub>-ATPase from *Escherichia coli* with mutant F<sub>O</sub> subunits. Partial purification and immunoprecipitation of F<sub>1</sub>F<sub>O</sub> complexes. *J. Biol. Chem.* 262:8340–8346.
49. Paule CR, Fillingame RH. 1989. Mutations in three of the putative transmembrane helices of subunit *a* of the *Escherichia coli* F<sub>1</sub>F<sub>O</sub>-ATPase disrupt ATP-driven proton translocation. *Arch. Biochem. Biophys.* 274:270–284.
50. Eya S, Maeda M, Futai M. 1991. Role of the carboxyl terminal region of H<sup>+</sup>-ATPase (F<sub>O</sub>F<sub>1</sub>) *a* subunit from *Escherichia coli*. *Arch. Biochem. Biophys.* 284:71–77.
51. Mertens N, Remaut E, Fiers W. 1995. Tight transcriptional control mechanism ensures stable high-level expression from T7 promoter-based expression plasmids. *Biotechnology* 13:175–179.
52. Wilcox G. 1974. The interaction of L-arabinose and D-fucose with AraC protein. *J. Biol. Chem.* 249:6892–6894.
53. Lee SK, Chou HH, Pflieger BF, Newman JD, Yoshikuni Y, Keasling JD. 2007. Directed evolution of AraC for improved compatibility of arabinose- and lactose-inducible promoters. *Appl. Environ. Microbiol.* 73:5711–5715.
54. Schramm HC, Schneppe B, Birkenhäger R, McCarthy JEG. 1996. The promoter-proximal, unstable IB region of the *atp* mRNA of *Escherichia coli*: an independently degraded region that can act as a destabilizing element. *Biochim. Biophys. Acta* 1307:162–170.
55. Deckers-Hebestreit G, Altendorf K. 1992. Influence of subunit-specific antibodies on the activity of the F<sub>O</sub> complex of the ATP synthase of *Escherichia coli*. II Effects of subunit *c*-specific polyclonal antibodies. *J. Biol. Chem.* 267:12370–12374.
56. Solomon KA, Brusilow WSA. 1988. Effect of an *uncE* ribosome-binding site mutation on the synthesis and assembly of the *Escherichia coli* proton-translocating ATPase. *J. Biol. Chem.* 263:5402–5407.
57. Etzold C, Deckers-Hebestreit G, Altendorf K. 1997. Turnover number of *Escherichia coli* F<sub>O</sub>F<sub>1</sub> ATP synthase for ATP synthesis in membrane vesicles. *Eur. J. Biochem.* 243:336–343.
58. Matthies D, Haberstock S, Joos F, Dötsch V, Vonck J, Bernhard F, Meier T. 2011. Cell-free expression and assembly of ATP synthase. *J. Mol. Biol.* 413:593–603.
59. Uhlemann EME, Pierson HE, Fillingame RH, Dmitriev OY. 2012. Cell-free synthesis of membrane subunits of ATP synthase in phospholipid bicelles: NMR shows subunit *a* fold similar to the protein in the cell membrane. *Protein Sci.* 21:279–288.
60. Gumbiowski K, Pänke O, Junge W, Engelbrecht S. 2002. Rotation of the *c* subunit oligomer in EF<sub>O</sub>EF<sub>1</sub> mutant cD61N. *J. Biol. Chem.* 277:31287–31290.
61. Kurzer F, Douraghi-Zadeh K. 1967. Advances in the chemistry of carbodiimides. *Chem. Rev.* 67:107–152.
62. Eya S, Maeda M, Tomochika KI, Kanemasa Y, Futai M. 1989. Overproduction of truncated subunit *a* of H<sup>+</sup>-ATPase causes growth inhibition of *Escherichia coli*. *J. Bacteriol.* 171:6853–6858.
63. von Meyenburg K, Jørgensen BB, Michelsen O, Sørensen L, McCarthy JEG. 1985. Proton conduction by subunit *a* of the membrane-bound ATP synthase of *Escherichia coli* revealed after induced overproduction. *EMBO J.* 4:2357–2363.
64. Arechaga I, Miroux B, Runswick MJ, Walker JE. 2003. Over-expression of *Escherichia coli* F<sub>1</sub>F<sub>O</sub>-ATPase subunit *a* is inhibited by instability of the *uncB* gene transcript. *FEBS Lett.* 547:97–100.
65. Matten SR, Schneider TD, Ringquist S, Brusilow WSA. 1998. Identification of an intragenic ribosome binding site that affects expression of the *atpB* gene of the *Escherichia coli* proton-translocating ATPase (*unc*) operon. *J. Bacteriol.* 180:3940–3945.
66. Iwamoto A, Omote H, Hanada H, Tomioka N, Itai A, Maeda M, Futai M. 1991. Mutations in Ser<sup>174</sup> and the glycine-rich sequence (Gly<sup>149</sup>, Gly<sup>150</sup>, and Thr<sup>156</sup>) in the  $\beta$  subunit of *Escherichia coli* H<sup>+</sup>-ATPase. *J. Biol. Chem.* 266:16350–16355.
67. Moriyama Y, Iwamoto A, Hanada H, Maeda M, Futai M. 1991. One-step purification of *Escherichia coli* H<sup>+</sup>-ATPase (F<sub>O</sub>F<sub>1</sub>) and its reconstitution into liposomes with neurotransmitter transporters. *J. Biol. Chem.* 266:22141–22146.
68. Hilbers F, Eggers R, Pradela K, Friedrich K, Herkenhoff-Hesselmann B, Becker E, Deckers-Hebestreit G. Subunit  $\Delta$  is the key player for assembly of the H<sup>+</sup>-translocating unit of *Escherichia coli* F<sub>O</sub>F<sub>1</sub> ATP synthase. *J. Biol. Chem.*, in press.